analytical chemistry

Article

pubs.acs.org/ac

Nanocalorimetry-Coupled Time-of-Flight Mass Spectrometry: Identifying Evolved Species during High-Rate Thermal Measurements

Feng Yi,[†] Jeffery B. DeLisio,[‡] Michael R. Zachariah,*[,‡] and David A. LaVan*[,†]

[†]Materials Measurement Science Division, Material Measurement Laboratory, National Institute of Standards and Technology, Gaithersburg, Maryland 20899, United States

[‡]Department of Chemical and Biomolecular Engineering, and Department of Chemistry and Biochemistry, University of Maryland, College Park, Maryland 20742, United States

Supporting Information

ABSTRACT: We report on measurements integrating a nanocalorimeter sensor into a time-of-flight mass spectrometer (TOFMS) for simultaneous thermal and speciation measurements at high heating rates. The nanocalorimeter sensor was incorporated into the extraction region of the TOFMS system to provide sample heating and thermal information essentially simultaneously with the evolved species identification. This approach can be used to measure chemical reactions and evolved species for a variety of materials. Furthermore, since the calorimetry is conducted within the same proximal volume as ionization and ion extraction, evolved species detected are in a collision-free environment, and thus, the possibility exists to interrogate intermediate and radical species. We present measurements showing the decomposition of ammonium perchlorate, copper oxide nanoparticles, and sodium azotetrazolate. The rapid, controlled, and quantifiable heating rate capabilities of the nanocalorimeter coupled with the 0.1 ms temporal resolution of the TOFMS provides a new measurement capability and insight into high-rate reactions, such as those seen with reactive and energetic materials, and adsorption \desorption measurements, critical for understanding surface chemistry and accelerating catalyst selection.

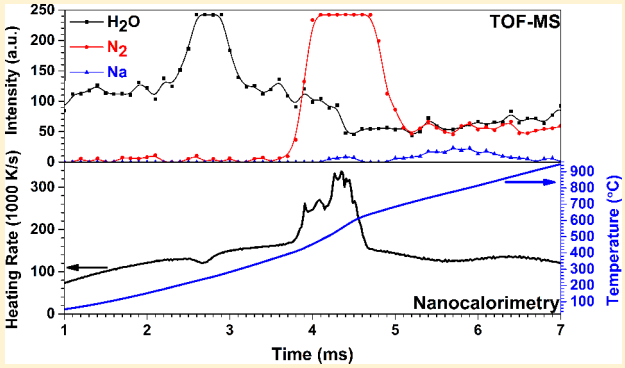

Temperature jump (T-jump) time-of-flight mass spectrometry (TOFMS) has previously been used for time-resolved speciation of rapidly heated materials.[1] This technique is capable of heating rates as high as ≈10^6 K/s up to a maximum temperature of around 1800 K.[2,3] These high heating rates coupled with rates of up to 20 000 spectra/s in the TOFMS can closely approximate a typical combustion event where temporally resolved temperature and speciation data can be obtained. However, T-jump TOFMS measurements lack the ability to quantify thermal properties (temperature, heat capacity, heat of reaction, etc.) to associate with the evolved species.

Microfabricated nanocalorimeter sensors are capable of making thermal measurements on samples with small mass (micrograms to nanograms), and at very fast heating and cooling rates.[4−8] Nanocalorimetry has been applied for measurements of a wide variety of types and forms of materials.[9] These dynamic thermal measurements can be made at rates up to 5 orders of magnitude faster than the traditional differential scanning calorimetry (DSC). A typical nanocalorimeter sensor can heat at rates up to 10^6 K/s and has sensitivity, in terms of heat capacity, on the order of 1 nJ/K. Figure 1a shows an image of the front of a typical nanocalorimeter that has a 100 nm thick platinum heater suspended on a 100 nm thick silicon nitride membrane in a silicon frame. The heating rate is sufficiently fast to take advantage of the rapid temporal resolution of the TOFMS.

Here, we report on the integration of nanocalorimetry with TOFMS to investigate dynamic thermal properties and evolved gaseous species to achieve (1) high sampling rates to capture dynamic processes and (2) simultaneous measurements of thermal properties and evolved chemical species. Here, three materials (an organic material, inorganic material, and a metal oxide nanoparticle) with different characteristics were selected to demonstrate the capability: specifically, sodium azotetrazolate, ammonium perchlorate, and copper oxide nanoparticles. The first two were electrosprayed onto the sensor using an appropriate solvent; the copper nanoparticles were dispersed in solution for electrospray. The Supporting Information provides details into the heat loss correction and heat capacity and enthalpy calculations in a nanocalorimeter experiment.

Received: May 19, 2015
Accepted: September 15, 2015
Published: September 15, 2015

DOI: 10.1021/acs.analchem.5b01872
Anal. Chem. 2015, 87, 9740−9744

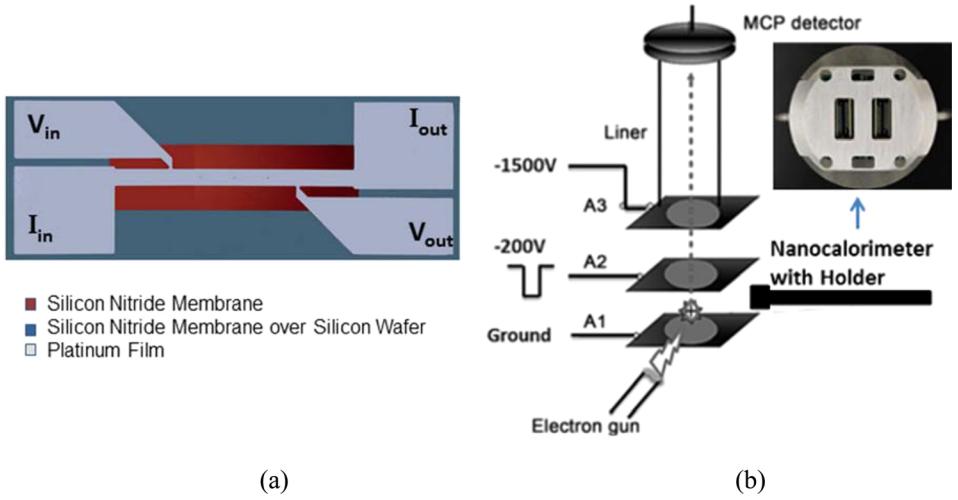

Figure 1. (a) Top view of a typical microfabricated nanocalorimeter sensor (13.7 mm long overall). (b) Schematic diagram of the nanocalorimeter integrated into the TOFMS with a photograph of the front face of the holder.

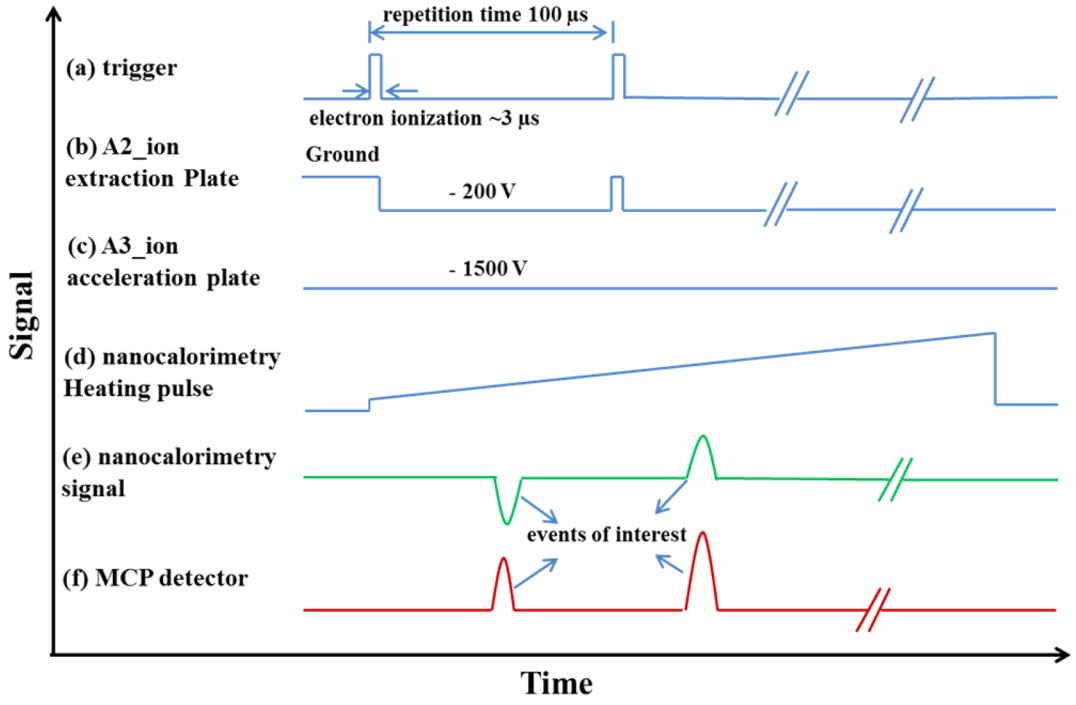

Figure 2. Synchronization scheme for integrated TOFMS and nanocalorimetry system.

EXPERIMENTAL SECTION

The nanocalorimeter sensors were inserted, using a custom holder, into the vacuum chamber of the mass spectrometer adjacent to the electron impact ionization region, as shown in Figure 1b.

The holder for the nanocalorimeter sensor was designed using commercially available ultrahigh-vacuum electrical and linear motion feedthroughs and a 3D-printed adapter and sensor cover. The thermoplastic material from the 3D printer provided little additional background signal and was satisfactory for initial measurements under high-vacuum conditions. Subsequent designs used components machined from poly(ether ether ketone) (PEEK) or aluminum. For TOFMS, the electron beam is normally operated at 70 eV and 1 mA, with the background pressure in the TOF chamber at $\approx 7 \times 10^{-5}$ Pa ($\approx 5 \times 10^{-7}$ Torr).[2,3] A linear TOFMS design of R. M. Jordan was used for these experiments. Specific details of the TOFMS system used have been previously described.[1−3] A 600 MHz oscilloscope (Teledyne Lecroy Waverunner 606Zi) was used for data acquisition in the TOFMS system. The oscilloscope was triggered at 10 kHz and ran using sequence mode with 95 segments, where each segment represents a mass spectrum; 50 μs of each segment was recorded with a 100×10^6 samples/s sampling rate.

The nanocalorimetry system can measure thermal signals at heating rates up to 10^6 K/s. The fabrication and calibration of the nanocalorimeter chips used in this work has been previously described in detail.[10] In brief, the calibration is based on resistive heating of the platinum heater/thermometer and optical pyrometry to record temperature. When using a Gaussian fit to identify peak centers, ref 10 shows that we identify the melting temperature for pure aluminum within 1 K

DOI: 10.1021/acs.analchem.5b01872
Anal. Chem. 2015, 87, 9740−9744

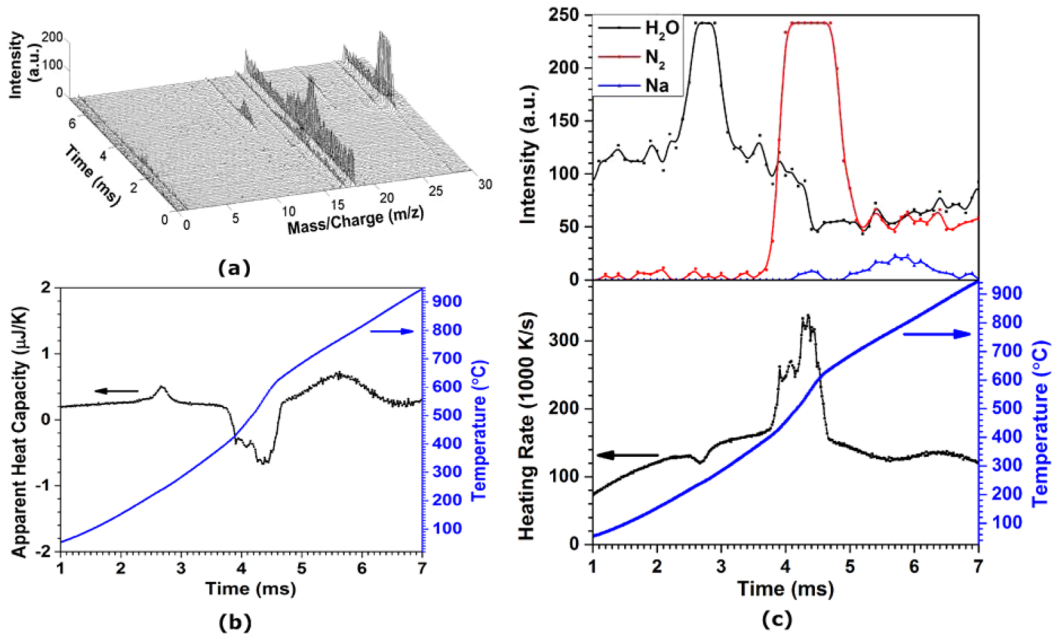

Figure 3. Results for sodium azotetrazolate (Na-TZ): (a) mass spectra, (b) nanocalorimetric thermal signals, (c) synchronized results of mass spectra and thermal analysis.

(at 933.5 K). The error associated with the temperature measurement is small and would be illegible if represented graphically on the plots presented here. Reference 10 does show highly detailed graphs and further analysis of error in repeated measurements. Measurements were performed by applying a current pulse and measuring the current and the voltage drop to provide an instantaneous measure of chip resistance and power. On the basis of the temperature coefficient of resistance from calibration, chip temperature is calculated at each data point (204×10^3 samples/s, ≈5 μs intervals). The acquired data is postprocessed to calculate apparent heat capacity by subtracting the heat losses found by examining the power needed to heat the bare chip. The term "apparent heat capacity" is used as this value includes contributions from the heat capacity of the sample and the enthalpy of the transformation(s) observed.

Synchronization between the TOFMS and nanocalorimetry system is critical in correlating the evolved species to the acquired thermal data. As shown in Figure 2, serial pulses generated from a pulse generator are used to trigger a high-voltage pulser so that the ionization and extraction processes occur continuously.

The data acquisition system for nanocalorimetry uses a PXI chassis with an embedded controller and two high-precision dynamic signal analysis cards (NI PXI-4461 and NI PXI-4462). This system can simultaneously generate two analog outputs and measuring six analog inputs with 24-bit resolution at speeds up to 204×10^3 samples/s. The PXI platform is also equipped with a precision clock for timing signals and triggering lines so that signal generation and measurement tasks can be synchronized with each other and external equipment like the TOFMS. The nanocalorimetry system does not start until the first trigger pulse is applied. Dynamic signal acquisition (DSA) devices use a digital filter to remove frequency components above the Nyquist frequency which introduces a filter delay, which for this hardware is 63 samples on inputs and 32 samples on outputs. Because we are synchronizing with another instrument, the filter delay for input has to be considered, so the delay is accounted for in recorded signals. The delay associated with ions traveling down the TOF tube is much shorter than the 5 μs interval between samples, so the ion travel delay was ignored for synchronization purposes.

The copper oxide nanoparticles and ammonium perchlorate used in this study were obtained from Sigma-Aldrich. The copper oxide nanoparticles had a nominal particle size of less than 50 nm. Sodium azotetrazolate was synthesized in house according to the reported procedure.[11]

RESULTS AND DISCUSSION

To demonstrate the capability of the integrated instrument, three different materials were measured including an organic salt, sodium azotetrazolate (Na-TZ), an inorganic compound, ammonium perchlorate (AP), and a metal oxide nanoparticle, copper oxide (CuO). The samples were deposited onto the nanocalorimeter sensor using electrospray.[12] During these experiments, the sample is heated for 8 ms and approximately 1600 data points are acquired at 5 μs intervals. Simultaneously, a sequence of 95 spectra with mass to charge ratio (m/z) up to 380 are recorded at 100 μs intervals. Trace background species observed when no samples were present in the TOFMS consist of H_2O^+, OH^+ (due to fragmentation of H_2O), N_2^+, and O_2^+.

Na-TZ is an energetic tetrazole salt that is fairly insensitive as a pentahydrate but is extremely sensitive and dangerous when it is dried.[11] These experiments were performed using the hydrated form of the salt. As shown in Figure 3, the mass spectrum shows the signal intensity of m/z ratios evolving with time (Figure 3a) and the nanocalorimetry results show temperature and apparent heat capacity/heating rate profiles of Na-Tz with time (Figure 3b). No high-mass ions were observed and major ions were only seen for $m/z < 30$. The mass spectra between 1 and 7 ms are plotted in Figure 3a. Three major species were observed: water, nitrogen, and sodium. The nanocalorimeter sensor (Figure 3b) measured three thermal signals. The most prominent feature is a large exotherm appearing at 4.3 ms, and 514 °C. At both 2.7 and 5.8

DOI: 10.1021/acs.analchem.5b01872
Anal. Chem. 2015, 87, 9740−9744

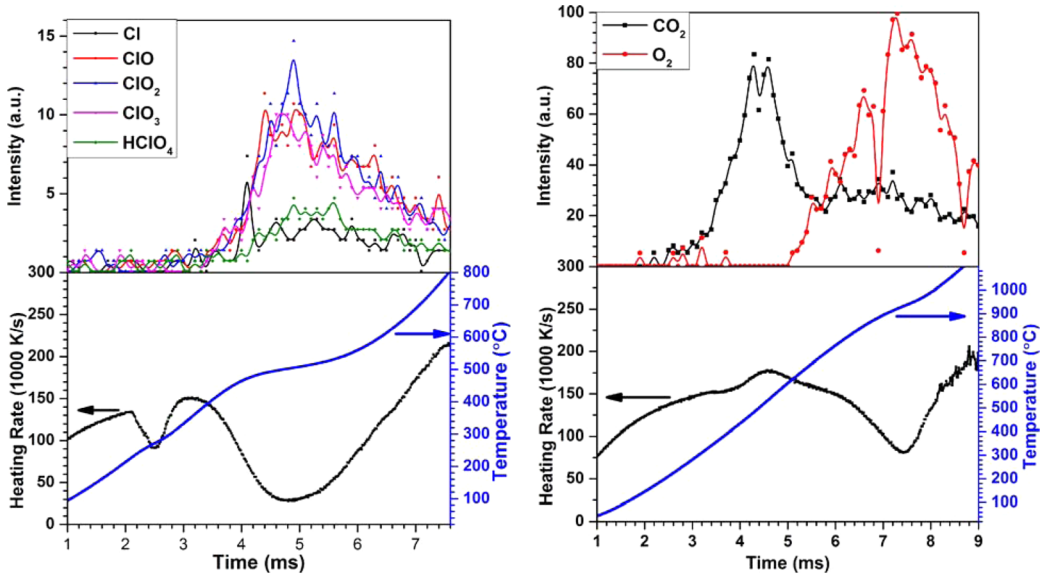

(a) (b)

Figure 4. Mass spectra and nanocalorimeter data: (a) ammonium perchlorate; (b) copper oxide.

ms, there are endotherms with corresponding temperatures of 238 and 774 °C, respectively. This measurement allows us to directly match the thermal results with the detected gas-phase species. As shown in Figure 3c, the first thermal signal at 2.7 ms (238 °C) is water from the dehydration of Na-Tz, which is an endothermic process. The large exotherm observed at 4.3 ms (514 °C) corresponds to the evolution of molecular nitrogen, from decomposition of Na-TZ. The proposed net decomposition reaction is shown below:

$$Na_2C_2N_{10} \rightarrow 5N_2 + 2C + 2Na$$

This decomposition is followed by an endotherm at 5.7 ms (770 °C) associated with the appearance of sodium. It should be noted that this temperature is significantly lower than the bulk boiling point of sodium (883 °C), likely due to volatilization under reduced pressure.

As a second example, we evaluate ammonium perchlorate (NH_4ClO_4), which is one of the most common oxidizers used in various propellants and pyrotechnics. Understanding the thermal decomposition of AP under combustion-like heating conditions is critical to understanding its combustion behavior. However, the thermal decomposition is complicated and strongly depends on experimental conditions such as whether it occurs in an open or closed system. This integrated instrument provides a new tool to measure and study thermal decomposition of AP. This experiment was performed under high vacuum (not an oxidizing environment); it reports on the initial decomposition, which would be one step to understanding the decomposition mechanism and subsequent reaction under oxidizing conditions.

In Figure 4a, we show results from rapid heating of AP. The endothermic peak at 2.5 ms (267 °C) in the AP results is attributed to the crystal transformation from orthorhombic to cubic form. After the phase transformation, a large endothermic signal appears which corresponds to evolution of ClO_2, $HClO_4$, ClO_3, ClO, and Cl as products of decomposition, which is similar to data recorded for the thermal decomposition of AP at approximately 400 °C.

As we mentioned briefly above, measurements on AP are highly sensitive to experimental conditions and material form. Under conditions where the reactants are readily transported away from the reaction (such as the measurement here, where a small sample is open to the vacuum chamber), the decomposition will be seen as endothermic, while exothermic decompositions will be seen for larger samples and those held in a sealed crucibles or under pressure. A difference that varies with test conditions, such as when using an open pan or sealed pan, has been reported previously for related macro scaled measurements.[13]

Ammonium perchlorate is known to have an exothermic decomposition when decomposed at temperatures above 380 °C and proceeds as follows:[14]

$$2NH_4ClO_4 \rightarrow Cl_2 + 2NO + O_2 + 4H_2O$$

In this experiment, it is proposed that gas-phase reactions are not occurring on the nanocalorimeter chip due to the nanocalorimeter being an open system at low pressure $\approx 1 \times 10^{-4}$ Pa ($\approx 10^{-6}$ Torr). These results agree with the previously proposed proton transfer based mechanism for decomposition of AP.[14] In the first step of this mechanism, there is proton transfer from cation to anion to form gaseous NH_3 and $HClO_4$. This is an endothermic, entropy-driven process. These gaseous species can then react to form the stable gaseous products described in the net equation above. Calculations using the National Aeronautics and Space Administration (NASA) Chemical Equilibrium with Applications (CEA) code were performed to validate that these gas-phase reactions are what make the overall decomposition reaction exothermic. For measurements in vacuum in an open calorimeter system, the gaseous species are unable to react and are ionized by the electron gun resulting in the mass spectrum and calorimeter results observed in this experiment.

Metal oxides, often in nanoparticle form, are often used as thermistors, chemical sensors, catalysts, and oxygen carriers for combustion reactions, such as in thermites or for chemical looping.[1,15−18] Here, copper oxide nanoparticles are electrosprayed onto the active area of the nanocalorimeter. Figure 4b

DOI: 10.1021/acs.analchem.5b01872
Anal. Chem. 2015, 87, 9740−9744

shows the mass spectra and thermal results. Two endothermic signals and the evolution of two species (CO_2 and O_2) were observed. At 3.8 ms (402 °C) an endothermic signal is observed corresponding to the release of CO_2 from decomposition of basic copper carbonate.[19] The second significantly larger endotherm at 7.4 ms (931 °C), shows significant evolution of molecular oxygen and indicates the decomposition of CuO. A large exothermic signal was also observed over 1100 °C accompanied by nitrogen release (data not shown), which may be related to the interaction between the released oxygen and sensor membrane.

Additional measurements on the same sample performed without breaking vacuum show a higher temperature peak corresponding to the melting of copper, which confirms the complete decomposition of copper oxide in the first cycle. The onset of the decomposition of copper oxide is at 5.0 ms (600 °C), which is slightly lower than a recent report[20] on the decomposition of copper oxide investigated using a T-jump TOFMS system that found the onset of oxygen release increases as the heating rate increases from $\approx 1.5 \times 10^5$ to $\approx 6.5 \times 10^5$ K/s. The corresponding onset temperature from that work would be at 650 °C, which is higher than the value reported here. There are slight differences in our method compared to this previous result—this sample is deposited in a more uniform, thin layer, and we individually calibrate each sensor, as the sensors are made from deposited platinum films.[21]

CONCLUSIONS

In summary, we presented the combination of nanocalorimetry and TOFMS as a novel integrated measurement capability to simultaneously measure thermal properties and evolved gas-phase speciation. This new technique expands on the previously described T-jump TOFMS technique by adding calorimetry capabilities while maintaining desirable high heating rates. Measurements for three different types of materials were presented to demonstrate the capability of the new instrument. A highly exothermic decomposition corresponding to the release of nitrogen gas was observed for the tetrazole salt, Na-TZ. CuO nanoparticles were also used as a test sample in which a measured endotherm could be coupled with the time-resolved TOFMS spectra to determine an oxygen release temperature. This system was also capable of probing the initial step in decomposition of AP where an endotherm and various gaseous species were identified. This method accelerates the investigation of material properties and the development of new applications, especially for energetic reactions and thermal desorption of catalytic materials.

ASSOCIATED CONTENT

Supporting Information

The Supporting Information is available free of charge on the ACS Publications website at DOI: 10.1021/acs.analchem.5b01872.

Summary of calculations necessary for nanocalorimetry measurements and additional Figures S-1 and S-2 (PDF)

AUTHOR INFORMATION

Corresponding Authors

*E-mail: mrz@umd.edu.
*E-mail: david.lavan@nist.gov.

Notes

Certain commercial equipment, instruments, or materials are identified in this document. Such identification does not imply recommendation or endorsement by the National Institute of Standards and Technology, nor does it imply that the products identified are necessarily the best available for the purpose. Fabrication performed in part at the NIST Center for Nanoscale Science & Technology (CNST).
The authors declare no competing financial interest.

ACKNOWLEDGMENTS

M.R.Z. and J.B.D. gratefully acknowledge the support of the Army Research Office and an AFOSR MURI.

REFERENCES

(1) Jian, G.; Piekiel, N. W.; Zachariah, M. R. *J. Phys. Chem. C* **2012**, *116*, 26881−26887.
(2) Zhou, L.; Piekiel, N.; Chowdhury, S.; Zachariah, M. R. *Rapid Commun. Mass Spectrom.* **2009**, *23*, 194−202.
(3) Zhou, L.; Piekiel, N.; Chowdhury, S.; Lee, D.; Zachariah, M. R. *J. Appl. Phys.* **2009**, *106*, 083306.
(4) Zhuravlev, E.; Schick, C. *Thermochim. Acta* **2010**, *505*, 1−13.
(5) Baldasseroni, C.; Queen, D. R.; Cooke, D. W.; Maize, K.; Shakouri, A.; Hellman, F. *Rev. Sci. Instrum.* **2011**, *82*, 093904.
(6) Lai, S. L.; Guo, J. Y.; Petrova, V.; Ramanath, G.; Allen, L. H. *Phys. Rev. Lett.* **1996**, *77*, 99−102.
(7) Carreto-Vazquez, V. H.; Wojcik, A. K.; Liu, Y. S.; Bukur, D. B.; Mannan, M. S. *Microelectron. J.* **2010**, *41*, 874−881.
(8) Yi, F.; Kim, I. K.; Li, S.; LaVan, D. A. *J. Pharm. Sci.* **2014**, *103*, 3442−3447.
(9) Yi, F.; LaVan, D. A. *Wiley interdisciplinary reviews. Nanomedicine and nanobiotechnology* **2012**, *4*, 31−41.
(10) Swaminathan, P.; Burke, B. G.; Holness, A. E.; Wilthan, B.; Hanssen, L.; Weihs, T. P.; LaVan, D. A. *Thermochim. Acta* **2011**, *522*, 60−65.
(11) Hiskey, M. A.; Goldman, N.; Stine, J. R. *J. Energ. Mater.* **1998**, *16*, 119−127.
(12) Yi, F.; LaVan, D. A. *Thermochim. Acta* **2013**, *569*, 1−7.
(13) Lesnikovich, A. I.; Ivashkevich, O. A.; Levchik, S. V.; Balabanovich, A. I.; Gaponik, P. N.; Kulak, A. A. *Thermochim. Acta* **2002**, *388*, 233−251.
(14) Boldyrev, V. V. *Thermochim. Acta* **2006**, *443*, 1−36.
(15) Adanez-Rubio, I.; Gayan, P.; Abad, A.; Garcia-Labiano, F.; de Diego, L. F.; Adanez, J. *Chem. Eng. J.* **2014**, *256*, 69−84.
(16) Podraza, N. J.; Gauntt, B. D.; Motyka, M. A.; Dickey, E. C.; Horn, M. W. *J. Appl. Phys.* **2012**, *111*, 073522.
(17) Miller, D. R.; Akbar, S. A.; Morris, P. A. *Sens. Actuators, B* **2014**, *204*, 250−272.
(18) Lee, D. W.; Yoo, B. R. *J. Ind. Eng. Chem.* **2014**, *20*, 3947−3959.
(19) Mansour, S. *J. Therm. Anal.* **1994**, *42*, 1251−1263.
(20) Jian, G.; Zhou, L.; Piekiel, N. W.; Zachariah, M. R. *ChemPhysChem* **2014**, *15*, 1666−1672.
(21) Yi, F.; Osborn, W.; Betz, J.; LaVan, D. A. *J. Microelectromech. Syst.* **2015**, *24*, 1185−1192.

DOI: 10.1021/acs.analchem.5b01872
Anal. Chem. 2015, 87, 9740−9744